



## **REINFORCED MASONRY CONCRETE BLOCK WALLS UNDER COMBINED AXIAL AND UNIFORMLY DISTRIBUTED LATERAL LOAD**

**Y. Llu<sup>1</sup>, J. Dawe<sup>2</sup> and D.Moxon<sup>3</sup>**

### **Abstract**

An experimental program consisting of laboratory testing of ten reinforced concrete masonry wall specimens was carried out to investigate their behaviour under combined axial and lateral loading. A computerized analytical technique, based on a finite element method, was developed to predict the behaviour of the walls. A moment - curvature relationship, developed to include effects of longitudinal reinforcing steel and masonry cracking, was used in the determination of wall element stiffnesses at successive load increments. Both experimental and analytical ultimate load capacities and effective flexural rigidities were obtained and compared with values suggested by the current Canadian CSA Standard S304.1-M94. The comparison indicates that the analytical technique gives a relatively accurate estimate of wall capacities and that existing code recommendations tend to underestimate the wall strength.

### **Key Words**

Masonry, walls, lateral load, slenderness.

### **1 Introduction**

Masonry load - bearing walls must be designed and constructed to perform safely, not always only under the action of gravity loads, but also frequently under the action of concentric or eccentric gravity loads in combination with lateral loads due to wind or earthquake. The interaction of axial loads and bending moments leads to complex design requirements that must include the combined interaction effects which comprise the so-called beam - column behaviour.

---

<sup>1</sup> Assistant Professor, Dept of Civil Engineering, Dalhousie University, Canada, yi.liu@dal.ca

<sup>2</sup> Professor, Dept of Civil Engineering, University of New Brunswick, Canada. Dawe@unb.ca.

<sup>3</sup> Graduate student, Dept of Civil Engineering, University of New Brunswick, Canada. Dmoxon@unb.ca.

The ultimate capacity of a beam - column is influenced not only by complex interaction of axial load and bending, but also by material behaviour as reflected by stress - strain relationships. The primary moment, which may be due to a gravity load acting through an eccentricity, to directly applied lateral loads, or to a combination of both, causes a primary lateral deflection which results in additional moment due to gravity load acting through this deflection. The additional moment results in additional deflection. The recurrent compounding effect of moment followed by deflection followed by moment is characteristic of the way in which beam - column action is described under the so-called P- $\Delta$  effect. This compounding effect of the axial load acting through lateral deflection results in the deepening of tension cracks in masonry. These in turn, reduce the effective moment of inertia,  $I$ , of the cross - section and elevate the level of stress thereby reducing the value of Young's modulus,  $E_m$ , which typically results from a non-linear masonry stress - strain constitutive relationship. Any attempt to accurately evaluate the effect of the interaction of axial compressive load and moment on the behaviour of masonry members prior to failure must consider the changes in  $E_m$  and  $I$  as stresses increase and tensile cracking occurs.

The currently applicable Canadian masonry design code (CSA S304.1 - M94) suggests using either a load - displacement (P- $\Delta$ ) method or a moment magnifier method to account for the compounding beam - column effect. While the P- $\Delta$  method is iterative and may require several successive calculations, the moment magnifier method accounts for the recurrent compounding beam - column effect in a single calculation by applying a magnification factor to the primary moment. An effective uniform flexural rigidity,  $EI_{eff}$ , is employed in both methods to include various effects of slenderness, stress increase, and tensile cracking at the ultimate strength limit state.

An experimental program was conducted to study the behaviour of masonry walls under combined axial and lateral loading. Test results were used to evaluate the effectiveness of using the moment magnifier method as currently recommended by the Canadian masonry code.

## 2 Previous research

Several authors have published notable work in this general area. Among these are Yokel et al. (1971), Fattal and Cattaneo (1976), Hatzinikolas and Warwaruk (1978), and Drysdale et al. (1993). While most of the analytical and experimental results were focused on walls under eccentric compressive loading, little is available on the subject of walls under combined axial and lateral out-of-plane loading.

The current Canadian masonry code, CSA Standard S304.1 - M94 (1994), recommends the following equation for calculating effective flexural rigidity for reinforced masonry:

$$(EI)_{eff} = E_m \left\{ 0.25I_0 - (0.25I_0 - I_{cr}) \left[ \frac{(e - e_k)}{2e_k} \right] \right\} \quad (1)$$

with the requirement that,  $E_m I_{cr} \leq (EI)_{eff} \leq 0.25E_m I_0$  where  $I_{cr}$  is the moment of inertia of the cracked section taken at yield and neglecting axial load effects, and  $e_k$  is the kern eccentricity. The effect of lateral loading is taken into account by using  $e$ , referred to as the virtual eccentricity, and evaluated as  $M_p / P_f$  where  $M_p$  and  $P_f$  are as defined previously.

The relevant literature shows a wide disparity among flexural rigidity values recommended by various researchers. Proposed equations have been either

empirically or semi-empirically founded with questionable agreement between experimental and theoretical results. Results of tests performed by Liu (2001) indicated that higher flexural rigidities exist in masonry walls that fail primarily by compression with only partial cracking of the sections. The use of a constant effective flexural rigidity for the entire length of a wall, which, in general, will develop variable depths and lengths of cracking zones is somewhat questionable. Based on these observations, the gathering of additional information on the determination of appropriate values of  $EI_{eff}$  is justified.

### 3 Experimental program

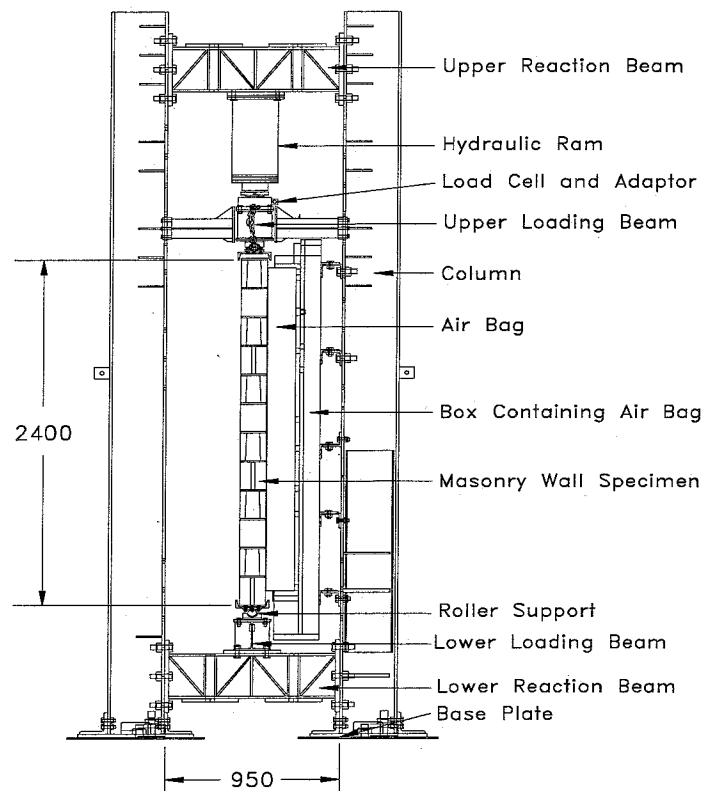
#### 3.1 Test specimens

Ten reinforced masonry walls were tested (Moxon, 2004) to evaluate the effect of axial pre-compression load combined with transverse uniformly distributed pressure on the strength of the walls. Standard two-core concrete masonry units of nominal thickness, 150 mm, were used for building the wall specimens which measured 990 mm long by 2400 mm high. Three 10M vertical reinforcing bars spaced at 400 mm were grouted into cells 200 mm from either edge of a wall specimen. Along with each test specimen, auxiliary tests were conducted to evaluate material properties of the masonry constituents, including blocks, mortar, grout and reinforcement.

#### 3.2 Experimental procedure

Several levels of axial pre-compression load were pre-determined based on considerations of the full spectrum of load vs. moment interaction of the cross-section strength. A pre-selected vertical load was applied first, slowly elevated to the desired value, and then maintained at a constant level while the lateral pressure applied by an air bag was gradually increased until failure occurred. In all wall tests, ultimate load was deemed to have occurred when the specimen displayed large lateral deflections at decreasing lateral load. In many cases, final failure was very explosive.

Figure 1 shows a self-equilibrating test frame consisting of four main members including two supporting columns, an upper loading beam, and a lower reaction beam. Vertical compressive loading was applied using an 1800 kN hydraulic ram secured to the top reaction beam as shown. Lateral pressure was applied by an air bag which was mounted inside a wooden reaction box. An electrical air pressure release valve was used to release the pressure at failure.



### 3.3 Instrumentation and data acquisition

Vertical loads, lateral loads, vertical deformations, and lateral deflections were measured and recorded by an automatic electronic multichannel data acquisition system. Both vertical and lateral loads were measured by strain gauge pressure transducers attached to in-line load cells. Each specimen was instrumented over its full height with rotary potentiometers calibrated to read linear deflections so that the vertical deflected wall profile could be monitored throughout the loading history. Two additional LSCs were mounted on the compressive face to provide an independent measurement of the average vertical deformation over the whole height of a specimen. Continuous load cell and deformation readings were taken during each test. Data acquisition and saving rates were set to 2 seconds.

### 3.4 Methodology

In a manner similar to that used by Yokel (1971), the model developed herein considers the simultaneous change of  $E$  and  $I$  as loads increase, by evaluating  $EI$  as a single quantity using the moment - curvature relationship:

$$EI = \frac{M}{\Phi} \quad (2)$$

where  $M$  is the total moment at a section including the moment – magnifier effect, and  $\Phi$  is the curvature of the section. For single curvature and pinned support conditions, cracking in a wall usually starts at a bed joint near mid-height where the total moment reaches a maximum and  $EI$  is at a minimum. The deflection profile of a wall specimen can be obtained based on lateral deflections measured along the full height of wall specimens. These values were used to compute  $\Phi$  using a finite difference technique.  $EI$  was then calculated with  $M$  expressed as  $(HL^2/8+P\Delta)$  where  $H$  and  $P$  are the applied lateral pressure and axial loads, respectively,  $L$  is the height of the specimen, and  $\Delta$  is mid-height deflection measured at the end of each load increment. The flexural rigidity is obtained as:

$$EI = \frac{(HL^2/8 + P\Delta)}{\Phi} \quad (3)$$

Lateral deflection along the full height of specimens were measured and recorded continuously during each test. The moment - curvature relationship was developed on the basis of values calculated using Eqns (2) and (3).

## 4 Numerical technique

### 4.1 Finite element model

In the research presented herein, a finite element method was used to simulate member behaviour and to investigate the variation of flexural rigidity along a member under increasing load. Since the analysis integrates the behaviour of individual elements, it is possible to track flexural rigidity and stress changes along the member and to provide realistic estimations of flexural rigidity and buckling capacity.

Priestly and Elder (1983) proposed a model for the stress - strain curves of grouted concrete masonry by modifying the Kent and Park curve for concrete. According to their results, this model showed good agreement with experimental data. Consequently, the Priestly and Elder model was adopted to estimate stress - strain curves for concrete masonry in compression.

The moment - curvature relationship was determined under specific axial force to evaluate the effective flexural rigidity as a single entity. However, because the stress - strain relationship of masonry is nonlinear in compression, the moment - curvature relationship cannot be found in an explicit form, and recourse must be made to numerical or empirical methods to obtain this relationship. Equilibrium conditions for a cross-section subjected to axial load and moment are used to establish a moment - curvature relationship which recognizes the nonlinear stress - strain nature of masonry in compression, the presence of steel reinforcing, and the effects of cracking. Thus, the effective rigidity as a function of moment and axial force can be obtained for each element.

The analytical method evaluates and integrates the behaviour of individual elements by tracking flexural rigidity changes and stress changes along a member thus providing realistic estimations of overall effective flexural rigidity, buckling capacity, and specimen response. In this procedure, a masonry wall is divided into  $m$  line elements of equal length along its height. Element stiffness matrices are determined and assembled into a structure stiffness matrix,  $[K]$ . Loads are assembled into a nodal force vector to establish an equilibrium equation of the form  $[K]\{w\} = \{F\}$  where  $\{w\}$  is a nodal displacement vector. At this point, boundary conditions may be applied and the resulting equations solved using a modified Cholesky method, for example. The technique adopted herein involves a process of incrementing external loads along positive stiffness portions of the loading curve and incrementing deflections when the stiffness is negative. During the process, failure checks are conducted at each load step and stiffness matrices are updated as required. This process is repeated until a complete load - deflection curve is obtained. Stability failure is checked as well as material failure. Calculation of the buckling load and lateral deflection includes the effects of modulus deterioration and cracking along the member at each load step. Using the calculated critical buckling load,  $P_{cr}$ , at failure, an effective flexural rigidity for the whole member can be determined as:

$$EI = \frac{P_{cr}(kh)^2}{\pi^2} \quad (4)$$

where  $k$  is the effective length factor and the other terms are as defined above.

## 4.2 Parametric study

Plain and single-layer reinforced walls subjected to both eccentric compressive loading and combined axial and lateral loading were considered. For eccentric compressive loading, the effects of slenderness, with values of  $h/t$  of 6, 12, 18, 24, 30 and 36, were used. Eccentricity ratios,  $e/t$ , with values of 0.1 to 1.0 with an increment of 0.1 for reinforced walls and 0.1 to 0.3 with an increment of 0.05 for plain walls were included. Moment gradients represented by  $e_1/e_2$  values of 1, 0, -1 were investigated.  $e_1/e_2 = 1$  defines single curvature bending while  $e_1/e_2 = -1$  indicates reverse curvature bending. For combined axial and lateral loading, the effect of slenderness ratios, with values of  $h/t = 6, 12, 18, 24, 30$ , and 36 was investigated. A wall with nominal cross-section thickness of 150 mm and length of 1 000 mm was used and pinned support conditions for both top and bottom of the wall were assumed. The load increment was 1 kPa and the tolerance of the convergence was set as 0.001 on the elements of successive load vectors. The number of iterations within the non-linear analysis was set at 200. The results of this extensive analytical study based on approximately 500 model tests yield two simplified bi-linear approximation curves for evaluating the effective flexural rigidities prior to failure for masonry beam-column elements (Liu and Dawe, 2003). These bi-linear approximations may be expressed as:

$$EI_{eff} / EI_0 = 1 - (2.375 - 0.0175 \frac{h}{t}) \frac{e}{t} \quad 0 \leq e/t < 0.4 \quad (5a)$$

$$EI_{eff} / EI_0 = 0.05 + 0.007 \frac{h}{t} \quad e/t \geq 0.4 \quad (5b)$$

The value of  $e$  in Eqn. (5) is equal to the maximum eccentricity for end applied axial loads. For combined axial and lateral loads,  $e$  is equal to  $M_p/P$  where  $M_p$  is the maximum primary moment and  $P$  is the axial load.

Verification of the analytical technique has been conducted by comparing analytical results with reported experimental findings including tests of walls under both eccentric loading and combined axial and lateral loading. The comparison shows that the analytical technique is capable of predicting the behaviour of masonry beam-columns with a broad range of physical properties and loading conditions (Liu, 2002)

## 5 Analysis and discussion of test results

### 5.1 Ultimate capacity

A summary of test results is given in Table 1. The mid-height deflections at the maximum lateral load were recorded and listed together with the maximum measured deflections. The experimentally obtained maximum moments carried by the specimens including P- $\Delta$  effects, are listed in the last column. Specimen W10 was tested under pure axial load reaching an ultimate value of 1663 kN. This value was used as a reference value when evaluating other specimens subjected to axial load and lateral pressure. Up to a sustained axial load level of 1000 kN, wall specimens showed increasing lateral load capacities accompanied by decreasing mid-height lateral deflections. For example, the lateral load capacity for Specimen W5 under an axial load of 600 kN was 39.7 kPa, which is 60 per cent above that of 24.7 kPa obtained as the average for specimens W1 and W2 tested under an axial load of 200 kN. The corresponding decrease in deflection was 47 per cent. For specimens reaching a tension failure mechanism, the effect of higher axial load on the increase in transverse strength outweighs the tendency of axial load, acting on the deflected shape, to cause a decrease in strength. This increase in strength, associated with tensile failure, coincides with the increasing part of the axial load vs. moment interaction diagram. However, for specimens tested under sustained axial loads above 1000 kN, the lateral load strength decreases as the failure mechanism shifts to one of compression as is reflected in the negative sloping portion of typical load vs. moment interaction diagrams. As shown in Table 1, for Specimen W7 tested under a sustained axial load of 1000 kN, the lateral load capacity was obtained as 50.3 kPa, which is in excess of the lateral load capacity of 44 kPa as obtained for a sustained axial load of 1400 kN for Specimen W9.

Three distinct observed failure modes include: (1) tension failure; (2) combined tension and compression failure; and (3) compression failure. For axial compressive loads up to approximately thirty five per cent of pure axial load capacity, the wall specimens failed by tensile cracking along horizontal joints near mid-height as shown in Figure 2. At about 50 to 60 per cent of ultimate lateral loading, visible horizontal cracks formed near the central mortar joint on the tension surface of the wall specimens. These cracks gradually penetrated into the wall thickness past the tensile steel. Shortly thereafter, local crushing occurred on the compressive face of the specimen at impending failure. Failure was gradual and occurred in a ductile manner. At about 80 to 90 per cent of ultimate lateral loading, visible horizontal cracks began forming between mortar joints and units on the tension face of wall specimens. The failure mechanism included

masonry crushing and spalling at both faces with vertical web splitting visible along the ends of the walls near the top and the bottom. Final collapse was complete and highly explosive as shown in Figure 3.

*Table 1 Summary of combined load test results of wall specimens*

| Specimen #  | Axial compressive load, P (kN) | Max. lateral pressure, $H_u$ , (kPa) | Mid-height deflection at max. lateral load (mm) | Max. mid-height deflection (mm) | Moment $M_{eu}$ (kN-m) |
|-------------|--------------------------------|--------------------------------------|---|---------------------------------|------------------------|
| W1          | 200                            | 26.8                                 | 26.2  | 61.0                            | 24.4                   |
| W2          | 200                            | 22.5                                 | 24.0  | 55.3                            | 20.9                   |
| <b>Mean</b> |                                | <b>24.7</b>                          | <b>25.1</b>                                     | <b>58.2</b>                     | <b>22.7</b>            |
| W3          | 400                            | 31.7                                 | 19.2  | 31.3                            | 30.2                   |
| W4          | 400                            | 34.0                                 | 20.4  | 36.7                            | 32.4                   |
| <b>Mean</b> |                                | <b>32.9</b>                          | <b>19.8</b>                                     | <b>34.0</b>                     | <b>31.3</b>            |
| W5          | 600                            | 39.7                                 | 13.2  | 36.6                            | 36.1                   |
| W6          | 800                            | 48.4                                 | 10.2  | 17.5                            | 42.7                   |
| W7          | 1000                           | 50.3                                 | 5.9   | 6.5                             | 41.8                   |
| W8          | 1200                           | 50.0                                 | 4.5   | 5.2                             | 40.5                   |
| W9          | 1400                           | 44.0                                 | 4.4   | 4.4                             | 35.8                   |
| W10         | 1663                           | 0                                    | ---   | ---                             | ---                    |



*Figure 2 Tension failure mode*



*Figure 3 Spalling of faceshells under high axial load*

In Figure 4, the set of curves of lateral load vs. mid-height lateral deflection show how specimens behave under increasing levels of sustained axial load. The figure shows that the lateral stiffness increases dramatically with the application of relatively low axial loads. As axial load increases, the lateral ductility decreases and the failure mechanism shifts to brittle behaviour in the range of axial load between forty and fifty per cent of the pure axial load capacity (1663 kN). When the axial load exceeds approximately sixty per cent (1000 kN) of the pure axial load capacity, the lateral capacity begins to decrease with increasing axial load and the failure mechanism becomes brittle and increasingly explosive. In Figures 5 and 6, the lateral pressure vs

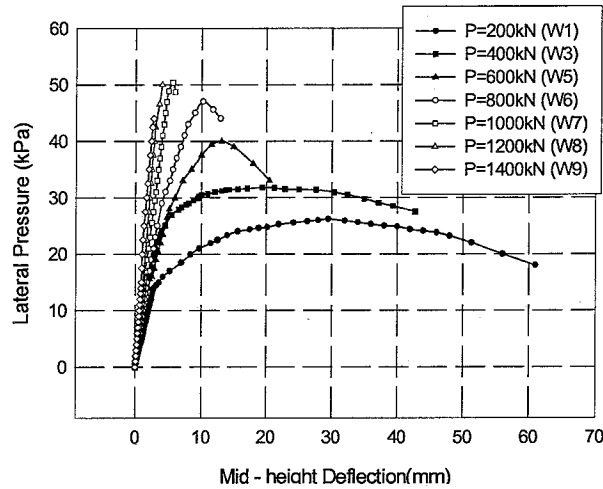


Figure 4 Load vs deflection curves for various tests

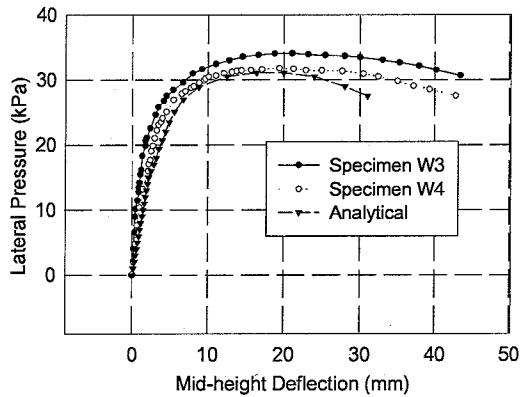


Figure 5 Comparison of analytical and experimental results ( $P=400\text{kN}$ )

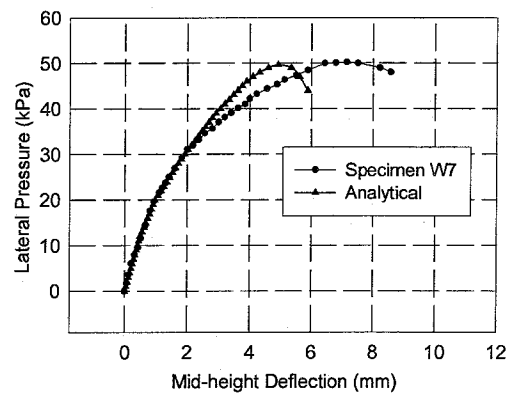


Figure 6 Comparison of analytical and experimental results ( $P=1000\text{kN}$ )

deflection curves obtained from analysis for axial load 400kN and 1000 kN are plotted together with experimental results. The comparison shows that the analytical method provides good agreement with experimental results.

## 5.2 Effective flexural rigidity

The effective flexural rigidities of wall specimens immediately prior to failure were obtained experimentally using Eqn. (3). The relationship between the effective flexural rigidity and eccentricity is shown in Figure 7 in which  $EI_o$  is the flexural rigidity for uncracked cross-sections and  $e/t$  is the ratio of equivalent loading eccentricity and the cross - section thickness. The lower and upper limits as recommended by the code are also indicated in the figure. A review of Figure 7 indicates that the analytical method provides a reasonable estimate of effective flexural rigidities immediately prior to failure. The Canadian design code and test values of  $EI_{eff}$  are in reasonable agreement for values of  $e/t \geq 0.4$ . As  $e/t$  decreases below 0.4, experimentally determined values of  $EI_{eff}$  increase markedly above corresponding values based on code determination. It should be kept in mind that  $e$  in the expression,  $e/t$ , is determined from the ratio of maximum primary moment to axial load. The underestimation of  $EI_{eff}$  values by the



Canadian design code is also reflected in Figure 8 where the experimental lateral pressure, including P- $\Delta$  effects, is plotted together with the values calculated using

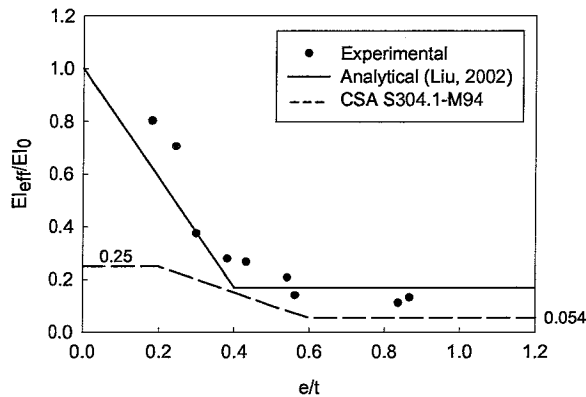


Figure 7 Comparison of  $E_{eff}/E_0$  vs  $e/t$  curves

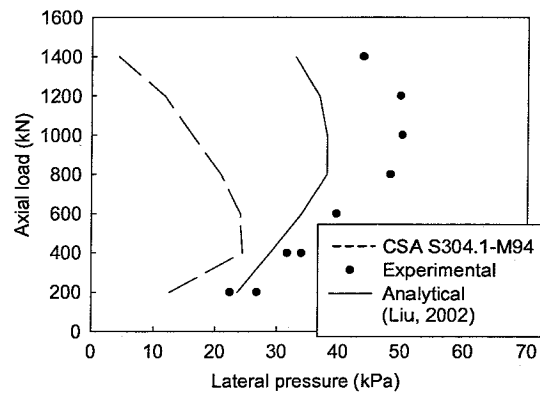


Figure 8 Comparison of axial load and lateral pressure interaction

both code and analytical equations. The figure indicates that the code, in general, underestimates the capacity of slender walls under combined axial and lateral load. This underestimation is most significant when combined compression and tension failure and compression failure are predominant. It is concluded that the code overestimates the P- $\Delta$  effects thus leading to a conservative design. The analytical solutions provide improved accuracy of the estimate of the wall capacities. It further demonstrates that the slenderness ratio affects  $E_{eff}$  and this effect should be reflected in the expression for the effective flexural rigidity.

## 6 Conclusions

The effective flexural rigidity of reinforced concrete masonry walls under combined axial and lateral loading has been experimentally investigated with the moment magnifier effect included in the determination of  $E_{eff}$ . A computerized analytical technique, based on a finite element method, was also developed to predict the behaviour of concrete masonry walls. A comparison of the values obtained from the analytical method with test results indicates that the analytical method provides encouraging accuracy of the estimates of ultimate capacity and effective flexural rigidity for walls under combined axial and lateral loading. The effective flexural rigidities prior to failure suggested by the Canadian masonry code were also calculated and compared with both experimental and analytical results. The comparison indicates that the code suggests more conservative values of effective flexural rigidity of masonry walls failing primarily by compression. It has been demonstrated that the effect of this appears to suggest that, in some regions of interaction, particularly where compression failure tends to be predominant, the code would require sections to be stronger than actually needed. To verify the analytical method, which has been developed for walls with any slenderness ratio and any combination of loadings, further experimental research including a broader spectrum of slenderness ratios and loading combinations is encouraged.

## References

- Fattal, S. G., and Cattaneo, L. E. 1976. Structural performance of masonry walls under compression and flexure. Building Science Series 73, National Bureau of Standards, Washington, D. C.

- Glanville, J., Hatzinikolas, M. A., and Ben-Omran, H. A. 1994. Engineered masonry design (Limit States Design). Canadian Standards Association, Rexdale, Ontario.
- Hatzinikolas, M. A., and Warwaruk, J. 1978. Concrete masonry walls. Structural Engineering Report No.70, Department of Civil Engineering, University of Alberta, Canada.
- Liu, Y., and Dawe, J. L. 2001. Experimental determination of masonry beam-column behaviour. Canadian Journal of Civil Engineering, **28**(3): 794-803.
- Liu, Y., and Dawe, J. L. 2003. Analytical modelling of masonry beam-column behaviour. Canadian Journal of Civil Engineering, **30**(5): 795-806.
- Liu, Y. 2002. Beam-column behaviour of masonry structural elements. Ph.D thesis, University of New Brunswick, Canada.
- Maksoud, A. A., and Drysdale, R. G. 1993. Rational moment magnification factor for slender unreinforced masonry walls. Proceedings of the 6<sup>th</sup> North American Masonry Conference, Vol. 1, pp.443-454.
- Moxon, Dana. 2004. Slender masonry walls under axial load and lateral uniformly distributed pressure. MScE thesis in progress, University of New Brunswick, Canada.
- Priestly, M. J. and Elder, D. M. 1983. Stress - strain curve for unconfined and confined concrete masonry, ACI Journal, **80**(3): 192-201.
- Yokel, F. Y., and Dikkers, R. D. 1971. Strength of load bearing masonry walls. Journal of the Structural Division, Proceedings of the American Society of Civil Engineers, pp. 1593-1609.